Erastin
[571203-78-6]

NB-64-08386-1mg

NB-64-08386-1mgx5

NB-64-08386-1mgx10

NB-64-08386-1mgx25

NB-64-08386-1mgx50

Erastin [571203-78-6]

#Cat: NB-64-08386-1mg Size: 1mg
#Cat: NB-64-08386-1mgx5 Size: 1mgx5
#Cat: NB-64-08386-1mgx10 Size: 1mgx10
#Cat: NB-64-08386-1mgx25 Size: 1mgx25
#Cat: NB-64-08386-1mgx50 Size: 1mgx50

Chemical Properties

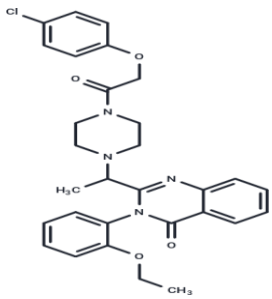

CAS No. : 571203-78-6
Formula : C30H31ClN4O4
Molecular Weight : 547.04
Appearance : Solid
Storage : Store at low temperature
Powder: -20°C for 3 years

Biological Description

Description	Erastin is an iron death activator that acts on the mitochondrial VDAC in a ROS- and iron- dependent manner. Erastin has anti-tumor activity and acts selectively on tumor cells with RAS-carcinogenic mutations.
Targets(IC50)	Ferroptosis, VDAC
In vitro	**METHODS:** Human gastric cancer cells HGC-27 were treated with Erastin (1-50 μM) for 24 h, and cell growth inhibition was detected by CCK-8. **RESULTS:** Erastin dose-dependently inhibited HGC-27 cell growth with an IC50 of approximately 14.39 μM. [1] **METHODS:** Human melanoma cells A375 were treated with Erastin (2-10 μM) for 3-12 h. The expression levels of target proteins were detected by Western Blot. **RESULTS:** Erastin treatment caused a significant down-regulation of VDAC2 and VDAC3, and a slight decrease of VDAC1 in A375 cells. [2] **METHODS:** Human colon cancer cells HT-29 were treated with Erastin (0.1-30 μM) for 12 h. The intracellular ROS levels were measured by Flow Cytometry. **RESULTS:** Erastin treatment significantly increased ROS levels in HT-29 cells. [3]
In vivo	**METHODS:** To test the antitumor activity in vivo, erastin (20 mg/kg in 20 μL DMSO plus 130 μL corn oil) was intraperitoneally injected into NSG mice bearing human prostate cancer tumors DU145, ARCaP, PC3, or H660 once daily for two to five weeks. **RESULTS:** Erastin treatment significantly inhibited the growth of human

	prostate cancer tumors, indicating antitumor activity in vivo. [4] **METHODS:** To study the effect of erastin treatment on anticancer radiation efficiency, erastin (15 mg/kg in 5% DMSO/corn oil) was injected intraperitoneally into BALB/c Slc- nu/nu mice bearing human lung adenocarcinoma tumor NCI-H1975 once a day for three days. Twenty-four hours after the last erastin injection, the anesthetized mice were locally irradiated with 3 Gy X-rays. **RESULTS:** Erastin-treated NCI-H1975 cell transplanted mice showed a trend of sensitization to X-ray irradiation with a concomitant decrease in intra-tumoral glutathione concentration. [5]
Cell Research	BJeLR cells were plated at 100,000 cells/dish in 35 mm tissue culture dishes. After 12h cells were treated with vehicle (DMSO; 10 hrs), erastin (37 µM; 10 hrs), staurosporine (750 nM; 8 hrs), hydrogen peroxide (16 mM; 1 hr) or rapamycin (100 nM; 24 hrs). Cells were fixed with 2.5% glutaraldehyde in 0.1 M Sorenson's buffer (0.1 M H2PO4, 0.1 M HPO4 (pH 7.2)) for at least 1 h, and then treated with 1% OsO4 in 0.1 M Sorenson's buffer for 1 h. Enblock staining used 1% tannic acid. After dehydration through an ethanol series, cells were embedded in Lx-112 and Embed-812 (EMS). Thin sections were cut on an MT-7000 ultramicrotome, stained with 1% uranyl acetate and 0.4% lead citrate, and examined under a Jeol JEM-1200 EXII electron microscope. Pictures were taken on an ORCA-HR digital camera at 5,000-50,000-fold magnification [1].
Animal Research	Tumor growth studies were performed in severe combined immunodeficient (SCID) mice xenograft model. Briefly, 2×10^6 viable HT-29 cells in 100 µL of growth medium (per mouse) were subcutaneously inoculated, and mice bearing ~100 mm3 tumors were randomly divided into three groups with 10 mice per group. Mice were treated daily with 10 or 30 mg/kg body weight of erastin (intraperitoneal injection, for 4 weeks) or vehicle control (Saline). Tumor volumes were calculated by the modified ellipsoid formula: (π / 6) ×AB2, where A is the longest and B is the shortest perpendicular axis of a tumor mass. Mice body weights were also recorded every week. Humane endpoints were always utilized to minimize mice suffering. Animals were observed on daily bases. Signs such as significant-reduced locomotion, severe diarrhea, severe piloerection or a sudden weight loss (> 20%) were recorded. If animals reached these endpoints they were euthanized by exsanguination under 2,2,2-tribromoethanol anesthesia (4 mg/10 g body weight). All injections were performed under the 2,2,2-tribromoethanol anesthesia method [3].

Solubility Information

Solubility	DMSO: 25 mg/mL (45.7 mM), Sonication is recommended. The compound is unstable in solution. Please use soon. Ethanol: < 1 mg/mL (insoluble or slightly soluble), 10% DMSO+40% PEG300+5% Tween 80+45% Saline: 1.6 mg/mL (2.92 mM),Solution.The compound is unstable in solution. Please use soon. H2O: < 1 mg/mL (insoluble or slightly soluble), (< 1 mg/ml refers to the product slightly soluble or insoluble)

Preparing Stock Solutions

	1mg	5mg	10mg
1mM	1.828 mL	9.1401 mL	18.2802 mL
5mM	0.3656 mL	1.828 mL	3.656 mL
10mM	0.1828 mL	0.914 mL	1.828 mL
50mM	0.0366 mL	0.1828 mL	0.3656 mL

Please select the appropriate solvent to prepare the stock solution, according to the solubility of the product in different solvents. Please use it as soon as possible.

Reference

Sun Y, et al. Erastin induces apoptotic and ferroptotic cell death by inducing ROS accumulation by causing mitochondrial dysfunction in gastric cancer cell HGC-27. Mol Med Rep. 2020 Oct;22(4):2826-2832.

Hu G, Cui Z, Chen X, et al.Suppressing Mesenchymal Stromal Cell Ferroptosis Via Targeting a Metabolism- Epigenetics Axis Corrects their Poor Retention and Insufficient Healing Benefits in the Injured Liver Milieu.Advanced Science.2023: 2206439.

Gartzke L P, Hendriks K D W, Hoogstra-Berends F, et al.Inhibition of Ferroptosis Enables Safe Rewarming of HEK293 Cells following Cooling in University of Wisconsin Cold Storage Solution.International Journal of Molecular Sciences.2023, 24(13): 10939.

Jiang X, Teng X, Shi H, et al.Discovery and optimization of olanzapine derivatives as new ferroptosis inhibitors. Bioorganic Chemistry.2023: 106393.

Liu J, Meng F, Lv J, et al.Comprehensive Monitoring of Mitochondrial Viscosity Variation during Different Cell Death Processes by a NIR Mitochondria-targeting Fluorescence Probe.Spectrochimica Acta Part A: Molecular and Biomolecular Spectroscopy.2023: 122602.

Tian Q, Zhou Y, Zhu L, et al. Development and validation of a ferroptosis-related gene signature for overall survival prediction in lung adenocarcinoma. Frontiers in Cell and Developmental Biology. 2021, 9.

Yan R, Xie E, Li Y, et al. The structure of erastin-bound xCT–4F2hc complex reveals molecular mechanisms underlying erastin-induced ferroptosis. Cell Research. 2022-32（7）P1-4

Kong R, Wang N, Han W, et al. IFNγ-mediated repression of system xc− drives vulnerability to induced ferroptosis in hepatocellular carcinoma cells. Journal of Leukocyte Biology. 2021, 110(2): 301-314.

Zheng Y, Kong F, Liu S, et al. Membrane protein-chimeric liposome-mediated delivery of triptolide for

targeted hepatocellular carcinoma therapy. Drug delivery. 2021
Tan Q, Fang Y, Peng X, et al. A new ferroptosis inhibitor, isolated from Ajuga nipponensis, protects neuronal cells via activating NRF2-antioxidant response elements (AREs) pathway. Bioorganic Chemistry. 2021: 105177.
Zhou Y, Wu H, Wang F, et al. GPX7 Is Targeted by miR-29b and GPX7 Knockdown Enhances Ferroptosis Induced by Erastin in Glioma. Frontiers in oncology. 2021, 11: 802124-802124.
Peng X, Tan Q, Wu L, et al. Ferroptosis Inhibitory Aromatic Abietane Diterpenoids from Ajuga decumbens and Structural Revision of Two 3, 4-Epoxy Group-Containing Abietanes. Journal of Natural Products. 2022
Yang Y, et al. Nedd4 ubiquitylates VDAC2/3 to suppress erastin-induced ferroptosis in melanoma. Nat Commun. 2020 Jan 23;11(1):433.
Li Y, Yang W, Zheng Y, et al.Targeting fatty acid synthase modulates sensitivity of hepatocellular carcinoma to sorafenib via ferroptosis.Journal of Experimental & Clinical Cancer Research.2023, 42(1): 1-19.
Li H, Shi W, Li X, et al. Ferroptosis is Accompanied by• OH Generation and Cytoplasmic Viscosity Increase Revealed via Dual-Functional Fluorescence Probe. Journal of the American Chemical Society. 2019
Zhu, Lizhe, et al. A novel ferroptosis-related gene signature for overall survival prediction in patients with breast cancer. Frontiers in Cell and Developmental Biology. 9 (2021)
Ning X, Qi H, Yuan Y, et al. Identification of a new small molecule that initiates ferroptosis in cancer cells by inhibiting the system Xc− to deplete GSH. European Journal of Pharmacology. 2022: 175304.
Kong R, Wang N, Han W, et al. IFNγ-mediated repression of system xc− drives vulnerability to induced ferroptosis in hepatocellular carcinoma cells. Journal of Leukocyte Biology. 2021, 110(2): 301-314.
Bi G, Liang J, Zhao M, et al. MiR-6077 promotes cisplatin/pemetrexed resistance in lung adenocarcinoma by targeting CDKN1A/cell cycle arrest and KEAP1/ferroptosis pathways. Molecular Therapy-Nucleic Acids. 2022
Yan B, Ai Y, Sun Q, et al. Membrane Damage during Ferroptosis Is Caused by Oxidation of Phospholipids Catalyzed by the Oxidoreductases POR and CYB5R1. Molecular Cell. 2020
Fang Y, Tan Q, Zhou H, et al. Discovery and optimization of 2-(trifluoromethyl) benzimidazole derivatives as novel ferroptosis inducers in vitro and in vivo. European Journal of Medicinal Chemistry. 2022: 114905.
Li P, Lin Q, Sun S, et al. Inhibition of cannabinoid receptor type 1 sensitizes triple-negative breast cancer cells to ferroptosis via regulating fatty acid metabolism. Cell Death & Disease. 2022, 13(9): 1-15.
Li H, Shi W, Li X, et al. Ferroptosis Accompanied by •OH Generation and Cytoplasmic Viscosity Increase Revealed via Dual-Functional Fluorescence Probe. Journal of the American Chemical Society. 2019, 141(45): 18301-18307
Wu Z, Geng Y, Lu X, et al. Chaperone-mediated autophagy is involved in the execution of ferroptosis. Proceedings of the National Academy of Sciences. 2019 Feb 19;116(8):2996-3005 Huo H, et al. Erastin Disrupts Mitochondrial Permeability Transition Pore (mPTP) and Induces Apoptotic Death of Colorectal Cancer Cells. PLoS One. 2016 May 12;11(5):e0154605.
Xiang P, Chen Q, Chen L, et al.Metabolite Neu5Ac triggers SLC3A2 degradation promoting vascular endothelial ferroptosis and aggravates atherosclerosis progression in ApoE-/-mice.Theranostics.2023, 13(14): 4993.
Wang J, Yan J T, Zeng S T, et al.Revealing Mitochondrion–Lysosome Dynamic Interactions and pH Variations in Live Cells with a pH-Sensitive Fluorescent Probe.Analytical Chemistry.2023
Li Z, Zhao B, Zhang Y, et al.Mitochondria-mediated ferroptosis contributes to the inflammatory responses of bovine viral diarrhea virus (BVDV) in vitro.Journal of Virology.2024: e01880-23.

Yang X, Li W, Li S, et al.Fish oil-based microemulsion can efficiently deliver oral peptide blocking PD-1/PD-L1 and simultaneously induce ferroptosis for cancer immunotherapy.Journal of Controlled Release.2024, 365: 654-667. Yin Z, Liu Q, Gao Y, et al.GOLPH3 promotes tumor malignancy via inhibition of ferroptosis by upregulating SLC7A11 in cholangiocarcinoma.Molecular Carcinogenesis.2024
Du Y, Zhou Y, Yan X, et al.APE1 inhibition enhances ferroptotic cell death and contributes to hepatocellular carcinoma therapy.Cell Death & Differentiation.2024: 1-16.
Tan Q, Wu D, Lin Y, et al.Identifying eleven new ferroptosis inhibitors as neuroprotective agents from FDA- approved drugs.Bioorganic Chemistry.2024: 107261.
Huang Q, Ru Y, Luo Y, et al.Identification of a targeted ACSL4 inhibitor to treat ferroptosis-related diseases.Science Advances.2024, 10(13): eadk1200.
Yin H, Hu X, Xie C, et al.A T-cell Inspired Sonoporation System Enhances Low-dose X-ray-mediated Pyroptosis and Radioimmunotherapy Efficacy by Restoring Gasdermin-E Expression.Advanced Materials.2024: e2401384- e2401384.
Zhang B W, Yang D, Li J T.Luteolin alleviates sorafenib-induced ferroptosis of BRL-3A cells through modulation of the Nrf2/GPX4 signaling pathway.Tradit Med Res.2024, 9(10): 55.
Zheng J, Wang Q, Chen J, et al.Tumor mitochondrial oxidative phosphorylation stimulated by the nuclear receptor RORγ represents an effective therapeutic opportunity in osteosarcoma.Cell Reports Medicine.2024
Chen C, Yang Y, Guo Y, et al.CYP1B1 inhibits ferroptosis and induces anti-PD-1 resistance by degrading ACSL4 in colorectal cancer.Cell Death & Disease.2023, 14(4): 271.
Ghoochani A, et al. Ferroptosis Inducers Are a Novel Therapeutic Approach for Advanced Prostate Cancer. Cancer Res. 2021 Mar 15;81(6):1583-1594.
Ru Y, Luo Y, Liu D, et al.Isorhamnetin alleviates ferroptosis-mediated colitis by activating the NRF2/HO-1 pathway and chelating iron.International Immunopharmacology.2024, 135: 112318.
Zhao G, Liang J, Zhang Y, et al.MNT inhibits lung adenocarcinoma ferroptosis and chemosensitivity by suppressing SAT1.Communications Biology.2024, 7(1): 680.
Feng H, Yu J, Xu Z, et al.SLC7A9 suppression increases chemosensitivity by inducing ferroptosis via the inhibition of cystine transport in gastric cancer.eBioMedicine.2024, 109: 105375.
Deng P, Silva M, Yang N, et al.Artemisinin inhibits neuronal ferroptosis in Alzheimer's disease models by targeting KEAP1.Acta Pharmacologica Sinica.2024: 1-12.
Chen L, Wu Y, Lv T, et al.Mesenchymal stem cells enchanced by salidroside to inhibit ferroptosis and improve premature ovarian insufficiency via Keap1/Nrf2/GPX4 signaling.Redox Report.2025, 30(1): 2455914.
In vivo vulnerabilities to GPX4 and HDAC inhibitors in drug-persistent versus drug-resistant BRAFV600E lung adenocarcinoma
Shibata Y, et al. Erastin, a ferroptosis-inducing agent, sensitized cancer cells to X-ray irradiation via glutathione starvation in vitro and in vivo. PLoS One. 2019 Dec 4;14(12):e0225931.
Zeng S T, Shao W, Yu Z Y, et al.Construction of a TICT-AIE-Integrated Unimolecular Platform for Imaging Lipid Droplet–Mitochondrion Interactions in Live Cells and In Vivo.ACS Sensors.2022
Zhu X, Huang N, Ji Y, et al.Brusatol induces ferroptosis in oesophageal squamous cell carcinoma by repressing GSH synthesis and increasing the labile iron pool via inhibition of the NRF2 pathway.Biomedicine & Pharmacotherapy.2023, 167: 115567.
Yan B, Ai Y, Sun Q, et al. Membrane Damage during Ferroptosis Is Caused by Oxidation of Phospholipids Catalyzed by the Oxidoreductases POR and CYB5R1[J]. Molecular Cell. 2020
Zhao G, Liang J, Shan G, et al.KLF11 regulates lung adenocarcinoma ferroptosis and chemosensitivity by suppressing GPX4.Communications Biology.2023, 6(1): 570.

Wang Y, Li B, Liu G, et al.Corilagin attenuates intestinal ischemia/reperfusion injury in mice by inhibiting ferritinophagy-mediated ferroptosis through disrupting NCOA4-ferritin interaction.Life Sciences.2023: 122176. Bow Y D, Ko C C, Chang W T, et al.A novel quinoline derivative, DFIQ, sensitizes NSCLC cells to ferroptosis by promoting oxidative stress accompanied by autophagic dysfunction and mitochondrial damage.Cancer Cell International.2023, 23(1): 1-11.